

LM-05K005  
January 26, 2005

---

---

# **Complete Solution of Elastica for a Clamped-Hinged Beam, and its Applications to a Carbon Nanotube**

Y Mikata

---

---

## **NOTICE**

This report was prepared as an account of work sponsored by the United States Government. Neither the United States, nor the United States Department of Energy, nor any of their employees, nor any of their contractors, subcontractors, or their employees, makes any warranty, express or implied, or assumes any legal liability or responsibility for the accuracy, completeness or usefulness of any information, apparatus, product or process disclosed, or represents that its use would not infringe privately owned rights.

# Complete solution of elastica for a clamped-hinged beam, and its applications to a carbon nanotube

by

Yozo Mikata  
Lockheed Martin  
Structural Mechanics Development  
P.O. Box 1072  
Schenectady, NY 12301

## Abstract

This paper treats an exact elastica solution for a clamped-hinged beam, and its applications to a carbon nanotube. Although the elastica has a long history, and the exact post-buckling solution for the Euler buckling problem has been known for at least 150 years, it seems that the elastica solution for a post-buckled clamped-hinged beam has never been obtained. Therefore, the exact solution obtained in this paper constitutes an addition to the existing family of elastica solutions. As an application of the results, a post-buckling analysis of a single wall carbon nanotube is studied. Also, a potential use of the post-buckling analysis of the carbon nanotube for the determination of its Young's modulus has been indicated.

## 1. Introduction

Determination of post-buckling deformation of a beam has many important practical applications in structural mechanics. The discovery of carbon nanotubes (Iijima, 1991; Iijima and Ichihashi, 1993) and its use as a structural as well as an electric material, and the use of beams in other micro- and nano- devices are going to require the post-buckling analysis for a variety of beams even further. An enormous amount of studies have already been conducted on various properties of the carbon nanotube (e.g., Falvo, et. al., 1997; Govindjee and Sackman, 1999; Iijima, 1996; Krishnan, et. al., 1998; Lourie, et. al., 1998; Lu, 1997; Overney, et. al., 1993; Ru, 2001; Saito, et. al., 1992; Wong, et. al., 1997; Yakobson, et. al., 1996; Yao and Lordi, 1998). Basic properties of carbon nanotubes are discussed in a book by Saito, Dresselhaus and Dresselhaus (1998). Some of the above studies are related to the buckling of carbon nanotubes (Yakobson, et. al., 1996; Falvo, et. al., 1997; Lourie, et. al., 1998; Ru, 2001). Three of them (Falvo, et. al., Lourie et. al., and Ru) use linear buckling (eigenvalue) analyses appropriate for the determination of the buckling load and the linear buckling mode, and the other one (Yakobson, et. al.) uses both molecular dynamics (MD) and a linear buckling (eigenvalue) analysis. However, it seems that a post-buckling analysis of a carbon nanotube has not received wide attention at this point except for the MD

calculation, which in principle is capable of producing the post-buckling shape. If we want to know the post-buckling shape, we need to perform the post-buckling analysis.

In this paper, the carbon nanotube is modeled as a beam, and the post-buckling analysis will be performed using continuum mechanics. Post-buckling analysis of a beam requires an exact analysis of the curvature, which is usually linearized in the pre-buckling analysis of a beam including the calculation of the critical buckling loads. When the curvature is treated exactly, the deformation analysis (and its solution) of a beam is called “elastica”. Elastica has a long history starting with Euler’s elastica (Euler, 1744; see also Timoshenko, 1983) for a horizontal cantilever subject to a vertical load at the end, and requires solving a nonlinear differential equation. According to Timoshenko (1983), Euler obtained the solution for his problem by using an infinite series in 1744. Euler investigated various types of elastica including column buckling in “De curvis elasticis (1744),” and in the limiting case, he obtained his famous buckling load formula. Later in 1759, Euler simplified the derivation of the linear buckling load. Exact elastica solution for a column buckling in terms of Jacobian elliptic functions (see Timoshenko and Gere, 1961) seems to have originated from Kirchhoff’s paper (1859) and the subsequent development (e.g., Clebsch, 1862; Hess, 1884 and 1885) based on Kirchhoff’s kinetic analogy (1859) of elastica with the motion of rigid body (see also Love, 1944). Comprehensive list of literature on large deflections of beams up to 1962 is provided by Frisch-Fay (1962). Even though the elastica of a post-buckled beam has been studied for a long time, it seems that most of the available solutions are for a statically determinate beam. To the best of author’s knowledge, no exact elastica solution has been obtained for a post-buckled clamped-hinged beam.

The main results of this paper are an exact elastica solution for a post-buckled clamped-hinged beam, and its applications to a carbon nanotube. In the following, the problem definition is given in Section 2, the elastica solution in Section 3, the numerical results and applications to the carbon nanotube in Section 4, and finally, the conclusion is given in Section 5.

## 2. Problem statement

Consider an originally straight beam which is deformed by the axial force  $P$  as shown in Fig. 1. One end is simply supported, and the other end is clamped. The axial force  $P$  is assumed to be sufficiently large so that the buckling of the beam is already caused. The objective of this paper is to determine the post-buckling deformation of the beam. The governing equation for the clamped-hinged beam shown in Fig. 1 is given by

$$EI \frac{d^2\theta}{ds^2} + P \sin \theta - R \cos \theta = 0 \quad (1)$$

where  $s$  is the arc length along the beam measured from the hinged end, and  $\theta$  is the angle between the tangent of the beam at  $s$  and the  $x$ -axis. Also  $E$  is the Young’s

modulus, and  $I$  is the moment of inertia of the cross section of the beam, and  $R$  is an unknown reaction force. Eq. (1) can be written as

$$\frac{d^2\theta}{ds^2} + b^2 \sin(\theta - \alpha) = 0 \quad (2)$$

where

$$b^2 = \frac{\sqrt{P^2 + R^2}}{EI} \quad (3)$$

$$\cos \alpha = \frac{P}{\sqrt{P^2 + R^2}} \quad (4)$$

$$\sin \alpha = \frac{R}{\sqrt{P^2 + R^2}}$$

Eq. (2) can be also written as

$$\frac{d^2\phi}{ds^2} + b^2 \sin \phi = 0 \quad (5)$$

where

$$\phi = \theta - \alpha \quad (6)$$

The relations between the arc length coordinate  $s$  and  $x, y$  coordinates are given by

$$\frac{dx}{ds} = \cos \theta \quad (7)$$

$$\frac{dy}{ds} = \sin \theta$$

The boundary conditions for this problem are given by

$$\theta(0) = \theta_0 \quad \theta(l) = 0 \quad (8)$$

$$\frac{d\theta}{ds}(0) = 0$$

$$y(0) = 0 \quad y(l) = 0 \quad (9)$$

By solving Eq. (5) under the boundary conditions (8) and (9) with the auxiliary relations (7),  $\theta(s)$ ,  $x(s)$ ,  $y(s)$ , and the reaction force  $R$  can be determined.

### 3. Elastica solution

Let us first rewrite Eq. (8) as

$$\begin{aligned}\phi(0) &= \phi_0 & \phi(l) &= -\alpha \\ \frac{d\phi}{ds}(0) &= 0\end{aligned}\tag{10}$$

where

$$\phi_0 = \theta_0 - \alpha\tag{11}$$

Let us set

$$v = \frac{d\phi}{ds}\tag{12}$$

Then (5) can be written as

$$\frac{1}{2} \frac{dv^2}{d\phi} + b^2 \sin \phi = 0\tag{13}$$

Integrating (13), we obtain

$$\frac{1}{2} v^2 - b^2 \cos \phi = C_1\tag{14}$$

where  $C_1$  is an integration constant. From (10) and (14), we obtain

$$C_1 = -b^2 \cos \phi_0\tag{15}$$

Substituting (15) into (14), we have

$$v^2 = 2b^2 (\cos \phi - \cos \phi_0)\tag{16}$$

From (12) and (16), we obtain

$$\frac{d\phi}{ds} = \pm b \sqrt{2(\cos \phi - \cos \phi_0)}\tag{17}$$

From Fig. 1, we have

$$\begin{aligned} \frac{d\phi}{ds} &= -b\sqrt{2(\cos\phi - \cos\phi_0)} & (0 < s < l^*) \\ \frac{d\phi}{ds} &= b\sqrt{2(\cos\phi - \cos\phi_0)} & (l^* < s < l) \end{aligned} \quad (18)$$

Integrating (18), we obtain

$$\int_0^{l^*} ds = -\int_{\phi_0}^{-\phi_0} \frac{d\phi}{b\sqrt{2(\cos\phi - \cos\phi_0)}} \quad (19-1)$$

$$\int_{l^*}^l ds = \int_{-\phi_0}^{-\alpha} \frac{d\phi}{b\sqrt{2(\cos\phi - \cos\phi_0)}} \quad (19-2)$$

From (19), we have

$$\begin{aligned} l^* &= \int_{-\phi_0}^{\phi_0} \frac{d\phi}{b\sqrt{2(\cos\phi - \cos\phi_0)}} \\ l - l^* &= \int_{-\phi_0}^{-\alpha} \frac{d\phi}{b\sqrt{2(\cos\phi - \cos\phi_0)}} \end{aligned} \quad (20)$$

From (20-1), we have

$$l^* = \frac{1}{b} \int_0^{\phi_0} \frac{d\phi}{\sqrt{\sin^2 \frac{\phi_0}{2} - \sin^2 \frac{\phi}{2}}} = \frac{2K(k)}{b} \quad (21)$$

where  $K(k)$  is the complete elliptic integral of the first kind, and  $k$  is a deformation parameter defined by

$$k = \sin \frac{\phi_0}{2} \quad (22)$$

From (20-2), we have

$$l - l^* = \frac{1}{2b} \int_{\alpha}^{\phi_0} \frac{d\phi}{\sqrt{\sin^2 \frac{\phi_0}{2} - \sin^2 \frac{\phi}{2}}} \quad (23)$$

Let us set

$$G(\alpha) = \int_{\alpha}^{\phi_0} \frac{d\phi}{\sqrt{\sin^2 \frac{\phi_0}{2} - \sin^2 \frac{\phi}{2}}} \quad (24)$$

Then we have

$$l - l^* = \frac{G}{2b} \quad (25)$$

Let us perform the following change of variables in (24).

$$\sin \lambda = \frac{\sin \frac{\phi}{2}}{\sin \frac{\phi_0}{2}} = \frac{1}{k} \sin \frac{\phi}{2} \quad (26)$$

$$\phi = \alpha \rightarrow \lambda = \lambda_{\alpha} \equiv \sin^{-1}\left(\frac{1}{k} \sin \frac{\alpha}{2}\right)$$

$$\phi = \phi_0 \rightarrow \lambda = \pi/2 \quad (27)$$

$$d\phi = \frac{2k \cos \lambda}{\cos \frac{\phi}{2}} d\lambda = \frac{2k \cos \lambda}{\sqrt{1 - k^2 \sin^2 \lambda}} d\lambda$$

Substituting (26) and (27) into (24), we have

$$\begin{aligned} G &= \frac{1}{k} \int_{\lambda_{\alpha}}^{\frac{\pi}{2}} \frac{1}{\sqrt{1 - \sin^2 \lambda}} \frac{2k \cos \lambda}{\sqrt{1 - k^2 \sin^2 \lambda}} d\lambda = 2 \int_{\lambda_{\alpha}}^{\frac{\pi}{2}} \frac{d\lambda}{\sqrt{1 - k^2 \sin^2 \lambda}} \\ &= 2 \left[ K(k) - \int_0^{\lambda_{\alpha}} \frac{d\lambda}{\sqrt{1 - k^2 \sin^2 \lambda}} \right] \end{aligned} \quad (28)$$

From the definition of the elliptic integral of the first kind,  $F(z, k)$ , we have

$$\int_0^{\lambda_{\alpha}} \frac{d\lambda}{\sqrt{1 - k^2 \sin^2 \lambda}} = F(\lambda_{\alpha}, k) = \operatorname{sn}^{-1}(\sin \lambda_{\alpha}, k) = \operatorname{sn}^{-1}\left(\frac{1}{k} \sin \frac{\alpha}{2}, k\right) \quad (29)$$

where  $\operatorname{sn}^{-1}(u, k)$  is an inverse Jacobian elliptic function. Substituting (29) into (28), we have

$$G(\alpha) = 2[K(k) - F(\lambda_\alpha, k)] = 2\left[K(k) - \operatorname{sn}^{-1}\left(\frac{1}{k} \sin \frac{\alpha}{2}, k\right)\right] \quad (30)$$

Substituting (21) and (30) into (25), we obtain

$$l = l^* + \frac{1}{b} \left[ K(k) - \operatorname{sn}^{-1}\left(\frac{1}{k} \sin \frac{\alpha}{2}, k\right) \right] = \frac{1}{b} \left[ 3K(k) - \operatorname{sn}^{-1}\left(\frac{1}{k} \sin \frac{\alpha}{2}, k\right) \right] \quad (31)$$

The above equation is one of the equations to be solved in our problem. Before manipulating the above equation to solve it, set us obtain the other equation for our problem. From (18), we have

$$\begin{aligned} ds &= -\frac{d\phi}{b\sqrt{2(\cos \phi - \cos \phi_0)}} & (0 < s < l^*) \\ ds &= \frac{d\phi}{b\sqrt{2(\cos \phi - \cos \phi_0)}} & (l^* < s < l) \end{aligned} \quad (32)$$

From (7-2) and (32), we have

$$y(l^*) = \int_0^{l^*} \sin \theta ds = \int_{-\phi_0}^{\phi_0} \frac{\sin(\phi + \alpha)}{b\sqrt{2(\cos \phi - \cos \phi_0)}} d\phi = \frac{2 \sin \alpha}{b\sqrt{2}} \int_0^{\phi_0} \frac{\cos \phi}{\sqrt{\cos \phi - \cos \phi_0}} d\phi \quad (33)$$

Similarly, we obtain

$$\begin{aligned} y(l) - y(l^*) &= \int_{-\phi_0}^{-\alpha} \frac{\sin(\phi + \alpha)}{b\sqrt{2(\cos \phi - \cos \phi_0)}} d\phi \\ &= \frac{\cos \alpha}{b\sqrt{2}} \int_{-\phi_0}^{-\alpha} \frac{\sin \phi}{\sqrt{\cos \phi - \cos \phi_0}} d\phi + \frac{\sin \alpha}{b\sqrt{2}} \int_{-\phi_0}^{-\alpha} \frac{\cos \phi}{\sqrt{\cos \phi - \cos \phi_0}} d\phi \end{aligned} \quad (34)$$

Let us set

$$\begin{aligned} I &= \int_{-\phi_0}^{-\alpha} \frac{\sin \phi}{\sqrt{\cos \phi - \cos \phi_0}} d\phi \\ J &= \int_{-\phi_0}^{-\alpha} \frac{\cos \phi}{\sqrt{\cos \phi - \cos \phi_0}} d\phi \end{aligned} \quad (35)$$



$$L = \int_0^{\phi_0} \frac{\cos \phi}{\sqrt{\cos \phi - \cos \phi_0}} d\phi$$

From (34) and (35), we obtain

$$y(l) = \frac{\cos \alpha}{b\sqrt{2}} I + \frac{\sin \alpha}{b\sqrt{2}} J + \frac{2 \sin \alpha}{b\sqrt{2}} L \quad (36)$$

From (35-3), we have

$$L = \int_0^{\phi_0} \frac{\cos \phi}{\sqrt{2 \left( \sin^2 \frac{\phi_0}{2} - \sin^2 \frac{\phi}{2} \right)}} d\phi = \sqrt{2} \int_0^{\frac{\pi}{2}} \frac{\cos \phi}{\cos \frac{\phi}{2}} d\lambda = \sqrt{2} [2E(k) - K(k)] \quad (37)$$

where the same change of variables, Eq. (26), was used, and  $E(k)$  is the complete elliptic integral of the second kind. From (35-1), we have

$$\begin{aligned} I &= -\sqrt{2} \int_{\lambda_\alpha}^{\frac{\pi}{2}} \frac{\sin \phi}{\cos \frac{\phi}{2}} d\lambda = -2\sqrt{2} \int_{\lambda_\alpha}^{\frac{\pi}{2}} \sin \frac{\phi}{2} d\lambda = -2\sqrt{2} k \int_{\lambda_\alpha}^{\frac{\pi}{2}} \sin \lambda d\lambda = -2\sqrt{2} k \cos \lambda_\alpha \\ &= -2\sqrt{2} \sqrt{k^2 - \sin^2 \frac{\alpha}{2}} \end{aligned} \quad (38)$$

Similarly from (35-2), we have

$$\begin{aligned} J &= \sqrt{2} \int_{\lambda_\alpha}^{\frac{\pi}{2}} \frac{\cos \phi}{\cos \frac{\phi}{2}} d\lambda = \sqrt{2} \left[ 2 \int_{\lambda_\alpha}^{\frac{\pi}{2}} \sqrt{1 - k^2 \sin^2 \lambda} d\lambda - \int_{\lambda_\alpha}^{\frac{\pi}{2}} \frac{d\lambda}{\sqrt{1 - k^2 \sin^2 \lambda}} \right] \\ &= \sqrt{2} [2(E(k) - E(\lambda_\alpha, k)) - (K(k) - F(\lambda_\alpha, k))] \\ &= \sqrt{2} [2E(k) - K(k) - (2E(\lambda_\alpha, k) - F(\lambda_\alpha, k))] \end{aligned} \quad (39)$$

where  $E(z, k)$  is the elliptic integral of the second kind. From (9) and (36) we have

$$\frac{1}{\sqrt{2}} [I \cos \alpha + J \sin \alpha + 2L \sin \alpha] = 0 \quad (40)$$

Substituting (37), (38), and (39) into (40), we finally obtain

$$\sin \alpha [3\{2E(k) - K(k)\} - \{2E(\lambda_\alpha, k) - F(\lambda_\alpha, k)\}] - 2 \cos \alpha \sqrt{k^2 - \sin^2 \frac{\alpha}{2}} = 0 \quad (41)$$

Eqs. (31) and (41) constitute a pair of transcendental equations for  $k$  and  $\alpha$ . These are highly nonlinear equations. Before going any further, let us write down the definitions of complete and incomplete elliptic integrals of the first kind and the second kind as well as the Jacobian elliptic functions below.

$$\begin{aligned}
 K(k) &= \int_0^{\frac{\pi}{2}} \frac{d\theta}{\sqrt{1-k^2 \sin^2 \theta}} \\
 E(k) &= \int_0^{\frac{\pi}{2}} \sqrt{1-k^2 \sin^2 \theta} d\theta
 \end{aligned}
 \tag{42}$$

$$F(\phi, k) = \int_0^{\phi} \frac{d\theta}{\sqrt{1-k^2 \sin^2 \theta}}$$

$$E(\phi, k) = \int_0^{\phi} \sqrt{1-k^2 \sin^2 \theta} d\theta$$

$$u = \int_0^x \frac{dx}{\sqrt{(1-x^2)(1-k^2 x^2)}} \quad (-1 \leq x \leq 1) \quad \leftrightarrow \quad x = \text{sn}(u, k)$$

$$cn(u, k) = \sqrt{1 - \text{sn}^2(u, k)} \tag{43}$$

$$dn(u, k) = \sqrt{1 - k^2 \text{sn}^2(u, k)}$$

Let us also introduce a non-dimensional load parameter  $\beta$  defined as

$$\beta = \sqrt{\frac{Pl^2}{EI}} \tag{44}$$

From (3), (4) and (44), we have

$$bl = \beta \sqrt{\sec \alpha} \tag{45}$$

By using (42) and (45), Eqs. (31) and (41) can be rewritten as

$$\beta \sqrt{\sec \alpha} = 3K(k) - \int_0^{\sin^{-1}(\frac{1}{k} \sin \frac{\alpha}{2})} \frac{dt}{\sqrt{1-k^2 \sin^2 t}}$$

$$\sin \alpha \left[ 3\{2E(k) - K(k)\} - 2 \int_0^{\sin^{-1}(\frac{1}{k} \sin \frac{\alpha}{2})} \sqrt{1 - k^2 \sin^2 t} dt + \int_0^{\sin^{-1}(\frac{1}{k} \sin \frac{\alpha}{2})} \frac{dt}{\sqrt{1 - k^2 \sin^2 t}} \right] - 2 \cos \alpha \sqrt{k^2 - \sin^2 \frac{\alpha}{2}} = 0 \quad (46)$$

Eq. (46) has to be solved for  $k$  and  $\alpha$  for a given  $\beta$ . It should be noted that the solution to the above equation represents a buckled solution. This means that the solution  $k = 0$  and  $\alpha = 0$  does not correspond to  $\beta = 0$ . In fact, it can be shown that the corresponding  $\beta$  is the smallest positive solution ( $\beta_{cr}$ ) of the following equation (see Appendix A).

$$\tan \beta = \beta \quad (47)$$

Eq. (47) is the same characteristic equation for the clamped-hinged beam as obtained from a linear buckling analysis. Thus we have recovered the result of the linear buckling analysis from our nonlinear analysis. The value of  $\beta_{cr}$  is given by

$$\beta_{cr} = 4.49341 \quad (48)$$

On the other hand, the original equation (1) together with the boundary conditions (8) and (9) permits the trivial solution for any value of  $P$  when  $\theta_0 = 0$ . The trivial solution is given by

$$\theta(s) = 0, \quad R = 0 \quad \text{for all } P \quad (49)$$

In order to solve (46), let us introduce another variable  $n$  defined as

$$n = \frac{\sin \frac{\alpha}{2}}{k} \quad (50)$$

By using (50), Eq. (46) can be rewritten as

$$\beta = \sqrt{1 - 2k^2 n^2} [3K(k) - sn^{-1}(n, k)] \quad (51-1)$$

$$\frac{n\sqrt{1 - k^2 n^2}}{1 - 2k^2 n^2} \left[ 3(2E(k) - K(k)) - 2 \int_0^{\sin^{-1} n} \sqrt{1 - k^2 \sin^2 t} dt + \int_0^{\sin^{-1} n} \frac{dt}{\sqrt{1 - k^2 \sin^2 t}} \right] - \sqrt{1 - n^2} = 0 \quad (51-2)$$

Eq. (51) has to be solved for  $k$  and  $n$  for a given  $\beta$ . Since this is a pair of transcendental equations, it has to be solved numerically. The way we proceed is as follows. First, (51-2) is solved for  $n(k)$  as a function of  $k$ . Once this is done, the relationship between  $k$  and  $\beta$  can be obtained from (51-1) as

$$\beta = \sqrt{1 - 2k^2 n(k)^2} \left[ 3K(k) - \int_0^{\sin^{-1} n(k)} \frac{dt}{\sqrt{1 - k^2 \sin^2 t}} \right] \quad (52)$$

If we want to obtain a specific value of  $k$  for a given  $\beta$ , we can solve (52) for  $k$  graphically or numerically. For most of the applications, the graphical solution is good enough. Once  $k$  and  $n(k)$  are determined for a given  $\beta$ ,  $\alpha$  and  $\theta_0$  are obtained as

$$\begin{aligned} \alpha &= 2 \sin^{-1}(nk) \\ \theta_0 &= 2[\sin^{-1} k + \sin^{-1}(nk)] \end{aligned} \quad (53)$$

By using (53), the reaction force  $R$  can be obtained as

$$R = P \tan \alpha = \frac{EI}{l^2} \beta^2 \tan \alpha \quad (54)$$

Let us now obtain  $\phi(s)$  as a function of  $s$ . Integrating (32-1), we obtain

$$\sqrt{2}bs = - \int_{\phi_0}^{\phi} \frac{d\phi}{\sqrt{\cos \phi - \cos \phi_0}} \quad (0 < s < l^*) \quad (55)$$

From (24), (30) and (55), we have

$$bs = \frac{G(\phi)}{2} = K(k) - sn^{-1}\left(\frac{1}{k} \sin \frac{\phi}{2}, k\right) \quad (0 < s < l^*) \quad (56)$$

Even though (56) is defined for  $s < l^*$ , it can be analytically continued for the whole domain ( $0 < s < l$ ). Eq. (56) can be inverted as

$$\sin \frac{\phi}{2} = k \operatorname{sn}(K(k) - bs, k) = k \operatorname{sn}(bs + K(k), k) \quad (0 < s < l^*) \quad (57)$$

where the first of the following properties of Jacobian elliptic functions is used.

$$\begin{aligned} \operatorname{sn}(u + 2K, k) &= -\operatorname{sn}(u, k) \\ \operatorname{cn}(u + 2K, k) &= -\operatorname{cn}(u, k) \\ \operatorname{dn}(u + 2K, k) &= \operatorname{dn}(u, k) \end{aligned} \quad (58)$$

Differentiating (57) with respect to  $s$ , we obtain

$$\frac{d\phi}{ds} = 2bk \operatorname{cn}(bs + K) \quad (59)$$

where some of the following properties of Jacobian elliptic functions are used.

$$\begin{aligned} \frac{d}{du} \operatorname{sn} u &= \operatorname{cn} u \operatorname{dn} u \\ \frac{d}{du} \operatorname{cn} u &= -\operatorname{sn} u \operatorname{dn} u \\ \frac{d}{du} \operatorname{dn} u &= -k^2 \operatorname{sn} u \operatorname{cn} u \end{aligned} \quad (60)$$

$$\operatorname{dn}^2 u + k^2 \operatorname{sn}^2 u = 1$$

$$\operatorname{sn}^2 u + \operatorname{cn}^2 u = 1$$

By using (59), the bending moment  $M(s, k)$  is obtained as

$$M(s, k) = EI \frac{d\theta}{ds} = EI \frac{d\phi}{ds} = 2EIbk \operatorname{cn}(bs + K) \quad (61)$$

A non-dimensional bending moment  $M^*(s, k)$  is defined as

$$M^*(s, k) \equiv \frac{M(s, k)}{Pl} = \frac{2EIbk}{Pl} \operatorname{cn}(bs + K) = \frac{2k}{\beta} \sqrt{\sec \alpha} \operatorname{cn}[K(k) + \beta \sqrt{\sec \alpha} \frac{s}{l}] \quad (62)$$

where  $\beta$  is defined in (44). Let us now integrate (7). From (7) together with the boundary conditions,  $x(0) = y(0) = 0$ , we have

$$\begin{aligned} x(s) &= \int_0^s \cos \theta ds = \int_0^s \cos(\phi + \alpha) ds = J(s) \cos \alpha - I(s) \sin \alpha \\ y(s) &= \int_0^s \sin \theta ds = \int_0^s \sin(\phi + \alpha) ds = I(s) \cos \alpha + J(s) \sin \alpha \end{aligned} \quad (63)$$

where

$$\begin{aligned} I(s) &= \int_0^s \sin \phi ds \\ J(s) &= \int_0^s \cos \phi ds \end{aligned} \quad (64)$$

By using (57), we have

$$\begin{aligned}\sin \phi &= 2k \operatorname{sn}(bs + K) \operatorname{dn}(bs + K) \\ \cos \phi &= 2 \operatorname{dn}^2(bs + K) - 1\end{aligned}\tag{65}$$

Substituting (65) into (64), we obtain

$$\begin{aligned}I &= 2k \int_0^s \operatorname{sn}(bs + K) \operatorname{dn}(bs + K) ds = -\frac{2k}{b} \operatorname{cn}(bs + K) \\ J &= 2 \int_0^s \operatorname{dn}^2(bs + K) ds - s = \frac{2}{b} \int_K^{bs+K} \operatorname{dn}^2 u du - s\end{aligned}\tag{66}$$

where the following integral formula was used.

$$\int \operatorname{sn} u \operatorname{dn} u du = -\operatorname{cn} u\tag{67}$$

Substituting (66) into (63), we finally obtain

$$\begin{aligned}x(s) &= \cos \alpha \left[ \frac{2}{b} L(s) - s \right] + \frac{2k}{b} \sin \alpha \operatorname{cn}(bs + K) \\ y(s) &= -\frac{2k}{b} \cos \alpha \operatorname{cn}(bs + K) + \sin \alpha \left[ \frac{2}{b} L(s) - s \right]\end{aligned}\tag{68}$$

where

$$L(s) = \int_K^{bs+K} \operatorname{dn}^2 u du\tag{69}$$

#### 4. Numerical results and applications to a carbon nanotube

The key result for our problem is the solution to Eq. (51), which provides the relationship between  $\beta$  and  $k$  given by (52). The numerical results for  $\beta(k)$  are shown in Fig. 2.

Similarly, the numerical results for  $\theta_0(k)$ ,  $\alpha(k)$  and  $\tan \alpha(k)$ , which can be obtained from (53), are shown in Figs. 3-5. It is interesting to note in Fig. 2 that there is a maximum value for  $\beta_{\max}$ , which is about 4.7968, when  $k \approx 0.6695$ . This means that the buckled

beam can accept the load up to  $\beta_{\max}^2 \frac{EI}{l^2}$ , and there is a physical instability beyond  $k =$

0.6695 ( $\equiv k_{\text{cr}}$ ). The value of  $\theta_0(k)$  at  $k = 0.6695$  is about 1.937 rad = 110°. After  $\theta_0(k)$  reaches 110°, the buckled beam continues to deform with a decreasing load  $P$

( $= \beta^2 \frac{EI}{l^2}$ ). The fact that there is a maximum value for  $\beta$  was not entirely obvious when

the analysis was initiated. It can be seen from Eq. (54) and Fig. 5 that, unlike the load  $P$ , the reaction force  $R$  continues to increase with  $k$  beyond  $k_{cr}$ .

Also, the non-dimensional bending moment  $M^*(s, k)$  as well as the coordinates  $(x(s), y(s))$  along the displacement curve can be obtained from Eqs. (62) and (68). The numerical results for  $M^*(s, k)$  and  $(x(s), y(s))$  when  $k = 0.3, 0.5, 0.7, 0.8$  are shown in Figs. 6-9. The physical instability mentioned above can be clearly seen in the deformed buckled shapes shown in Figs. 8-1 and 9-1, where  $\theta_0(k)$  is greater than  $110^\circ$ . It is also seen from Figs. 6-1, 7-1, 8-1, and 9-1 that the entire span of the beam in the  $x$ -direction continues to shrink as  $k$  increases. For example, when  $k = 0.7$ , the span of the beam in the  $x$ -direction has already shrunk more than 50%. At the same time, the lateral deflection reaches more than 30% of the length of the beam.

As an illustration of the application of the above results, let us consider a single wall carbon nanotube of radius  $r = 7\text{\AA}$ , thickness  $t = 3.4\text{\AA}$ , and length  $l = 30\text{ nm}$  under a compressive load  $P$  with clamped-hinged boundary conditions. Then the outer radius  $a$  and the inner radius  $b$  are given by  $a = 8.7\text{\AA}$ ,  $b = 5.3\text{\AA}$ . With these dimensions, the area moment of inertia  $I$  is calculated as  $I = 4.94 \times 10^{-37}\text{ m}^4$ . If we assume the Young's modulus  $E$  as  $E = 1000\text{ GPa}$ , the critical buckling load  $P_{cr}$  is calculated as  $P_{cr} = 1.11 \times 10^{-8}\text{ (N)}$ , where  $\beta_{cr} = 4.49341$  (see Eq. (48)) has been used. We notice that the critical buckling load is very small. Next, let us suppose that the carbon nanotube is already buckled with the deformation parameter  $k = 0.4$  (see Eq. (23)). Using Fig. 2, the corresponding  $\beta$  is obtained as  $\beta = 4.624$ . Then the required load  $P$  as well as the tip angle  $\theta_0$  are determined as  $P = 1.17 \times 10^{-8}\text{ (N)}$ ,  $\theta_0 = 1.021\text{ rad} = 58.5^\circ$ . It is seen from these calculations that as soon as the critical buckling load is reached, the deformation becomes very large very quickly. Now, we can also reverse the above procedure. If we happen to know the compressive load  $P$  and the tip angle  $\theta_0$ , then by using Figs. 2 and 3, we can determine the flexural rigidity  $EI$  of the carbon nanotube as follows.

$$k_0 = k(\theta_0) \Rightarrow \beta_0 = \beta_0(k_0) \Rightarrow EI = \frac{Pl^2}{\beta_0^2} \quad (70)$$

This indicates a potential use of the post-buckling analysis of the carbon nanotube for the determination of its Young's modulus.

## 5. Conclusion

This paper presents an exact elastica solution for the post-buckling analysis of a clamped-hinged beam, and its applications to a carbon nanotube. Although the elastica has a long history, and the exact solution for the Euler buckling problem has been known for about 150 years or maybe more, it seems that the elastica solution for a post-buckled clamped-hinged beam has never been obtained. Therefore, the present elastica solution constitutes a new addition to the existing list of elastica solutions (see Frisch-Fay, 1962). As part of the analysis, the characteristic equation of the linear

buckling analysis for the clamped-hinged beam is recovered from our nonlinear analysis. As an application of the results, a post-buckling analysis of a single wall carbon nanotube is treated. It is found that as soon as the critical buckling load is reached, the deformation becomes very large very quickly. Also, a potential use of the post-buckling analysis of the carbon nanotube for the determination of its Young's modulus has been indicated.



## References

1. Clebsch, Theorie der Elasticität fester Körper, Leipzig, (1862).
2. L. Euler, "Methodus inveniendi lineas curvas maximi minimive proprietate gaudentes...", Appendix I, "De curvis elasticis," Bousquet, Lausanne and Geneva, (1744).
3. L. Euler, "Sur la force des colonnes," Mem. Acad., Berlin, vol. 13, (1759).
4. M.R. Falvo, G.J. Clary, R.M. Taylor II, V. Chi, F.R. Brooks Jr., S. Washburn, and R. Superfine, "Bending and buckling of carbon nanotubes under large strain," Nature, vol. 389, pp. 582-584, (1997).
5. R. Frisch-Fay, Flexible Bars, Butterworth and Co., Ltd., (1962).
6. S. Govindjee and J.L. Sackman, "On the use of continuum mechanics to estimate the properties of nanotubes," Solid State Communications, 110, pp. 227-230, (1999).
7. E. Hernandez, C. Goze, P. Bernier, and A. Rubio, "Elastic properties of single-wall nanotubes," Applied Physics A, 68, pp.287-292, (1999).
8. W. Hess, Math. Ann., Bde. 23 (1884) and 25 (1885).
9. S. Iijima, "Helical microtubules of graphitic carbon," Nature, vol. 354, pp. 56-58, (1991).
10. S. Iijima, and T. Ichihashi, "Single-shell carbon nanotubes of 1-nm diameter," Nature, vol. 363, pp. 603-605, (1993).
11. S. Iijima, "Structural flexibility of carbon nanotubes," J. Chem. Phys. 104 (5), pp. 2089- 2092, (1996).
12. G.R. Kirchhoff, "Über das Gleichgewicht und die Bewegung eines unendlich dünnen elastischen Stabes," J. f. Math. (Crelle), Bd. 56, (1859).
13. A. Krishnan, E. Dujardin, T.W. Ebbesen, P.N. Yianilos, and M.M. Treacy, "Young's modulus of single-walled nanotubes," Phys. Rev. B, 58 (20), pp. 14013-14019, (1998).
14. O. Lourie, D.M. Cox, and H.D. Wagner, "Buckling and Collapse of Embedded Carbon Nanotubes," Phys. Rev. Lett., 81 (8), pp. 1638-1641, (1998).

15. A.E.H. Love, *A Treatise on the Mathematical Theory of Elasticity*, 4<sup>th</sup> Ed., Dover Publications, New York, (1944).
16. J.P. Lu, "Elastic Properties of Carbon Nanotubes and Nanoropes," *Phy. Rev. Lett.*, 79 (7), pp. 1297-1300, (1997).
17. G. Overney, W. Zjong, and D. Tomanek, "Structural rigidity and low frequency vibrational modes of long carbon tubules," *Z. Physik D*, 27, pp. 93-96, (1993).
18. C.Q. Ru, "Axially compressed buckling of doublewalled carbon nanotube embedded in an elastic medium," *J. Mech. Phys. Solids*, 49, pp. 1265-1279, (2001).
19. R. Saito, G. Dresselhaus, and M.S. Dresselhaus, *Physical Properties of Carbon Nanotubes*, Imperial College Press, London, (1998).
20. R. Saito, M. Fujita, G. Dresselhaus, and M.S. Dresselhaus, "Electronic structure of chiral graphene tubules," *Appl. Phys. Lett.* 60 (18), pp. 2204-2206, (1992).
21. S.P. Timoshenko and J.M. Gere, *Theory of Elastic Stability*, 2<sup>nd</sup> ed., McGraw-Hill, (1961).
22. S.P. Timoshenko, *History of Strength of Materials*, Dover Publications, New York, (1983).
23. E.W. Wong, P.E. Sheehan, and C.M. Lieber, "Nanobeam Mechanics: Elasticity, Strength, and Toughness of Nanorods and Nanotubes," *Science*, 277, pp. 1971-1975, (1997).
24. B.I. Yakobson, C.J. Brabec, and J. Bernholc, "Nanomechanics of Carbon Tubes: Instabilities beyond Linear Response," *Phys. Rev. Lett.*, 76 (14), pp. 2511-2514, (1996).
25. N. Yao and V. Lordi, "Young's modulus of single-walled carbon nanotubes," *J. Appl. Phys.*, 84 (4), pp. 1939-1943, (1998).
26. P. Zhang, Y. Huang, P.H. Geubelle, P.A. Klein, and K.C. Hwang, "The elastic modulus of single-wall carbon nanotubes: a continuum analysis incorporating interatomic potentials," *Inter. J. Solids Structures*, 39, pp. 3893-3906, (2002).

## Appendix A. Proof that the corresponding $\beta$ is non-zero

Let us use Eq. (51) instead of Eq. (46) for our purpose. Eq. (51) is written below for convenience.

$$\beta = \sqrt{1-2k^2n^2} [3K(k) - sn^{-1}(n, k)] \quad (\text{A1-1})$$

$$\begin{aligned} & \frac{n\sqrt{1-k^2n^2}}{1-2k^2n^2} \left[ 3(2E(k) - K(k)) - 2 \int_0^{\sin^{-1}n} \sqrt{1-k^2 \sin^2 t} dt + \int_0^{\sin^{-1}n} \frac{dt}{\sqrt{1-k^2 \sin^2 t}} \right] \\ & - \sqrt{1-n^2} = 0 \end{aligned} \quad (\text{A1-2})$$

We want to investigate the behavior of the above equation when  $k$  approaches zero. In the limit as  $k$  goes to zero, (A1) becomes

$$\begin{aligned} \beta &= \frac{3\pi}{2} - \sin^{-1} n \\ \frac{3\pi}{2} - \sin^{-1} n - \frac{\sqrt{1-n^2}}{n} &= 0 \end{aligned} \quad (\text{A2})$$

We want to show that  $\beta$  defined above is the smallest positive root of the following equation.

$$\tan \beta = \beta \quad (\text{A3})$$

It can be easily seen from (A2-1) that

$$\pi \leq \beta \leq 2\pi \quad (\text{A4})$$

since  $-\frac{\pi}{2} \leq \sin^{-1} n \leq \frac{\pi}{2}$ . Now, all we need to show is that  $\beta$  of (A2) satisfies (A3). From (A2), we have

$$n = \sin \left( \frac{3\pi}{2} - \frac{\sqrt{1-n^2}}{n} \right) = -\cos \frac{\sqrt{1-n^2}}{n} = -\cos \beta \quad (\text{A5})$$

From (A5), we obtain

$$\tan \beta = \sqrt{\sec^2 \beta - 1} = \sqrt{\frac{1}{\cos^2 \beta} - 1} = \frac{\sqrt{1-n^2}}{n} = \beta \quad (\text{A6})$$

since  $0 < n < 1$  from (A2-2). Q.E.D.

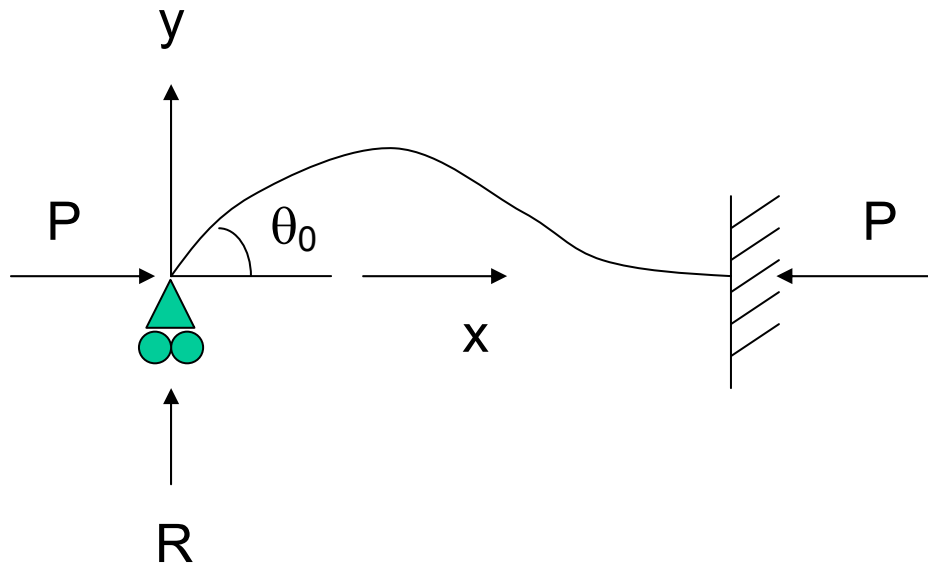
**Figures and Figure Captions**

Fig. 1. Clamped-hinged beam with Cartesian coordinates

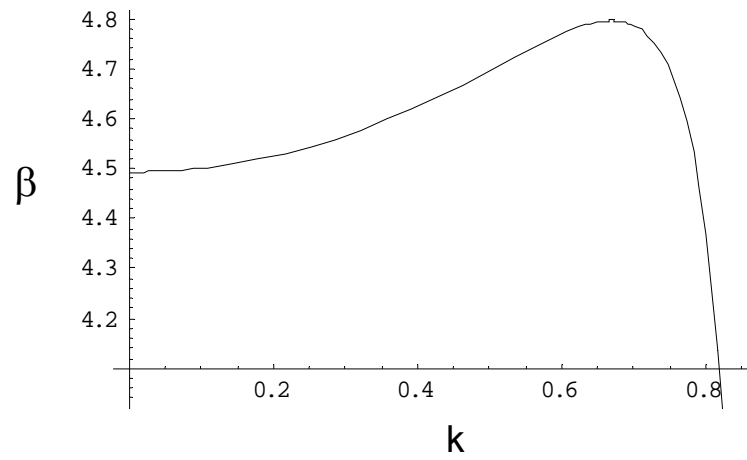


Fig. 2. Relationship between the load parameter  $\beta$  and the deformation parameter  $k$

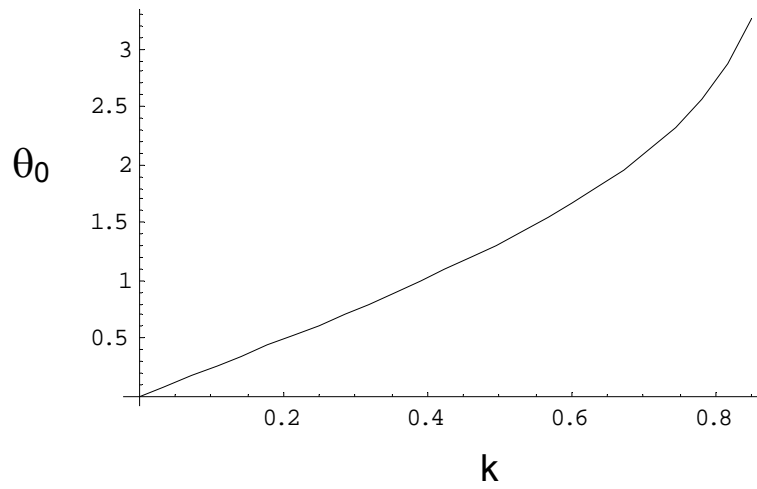


Fig. 3. Tip angle  $\theta_0$  as function of  $k$

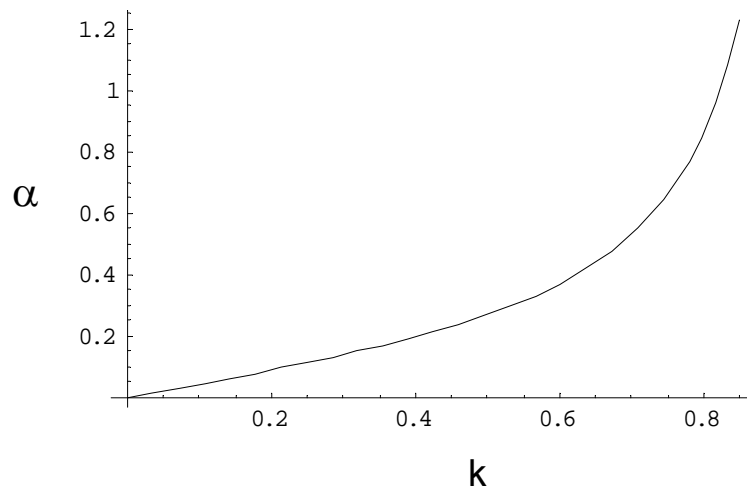


Fig. 4.  $\alpha$  as a function of  $k$

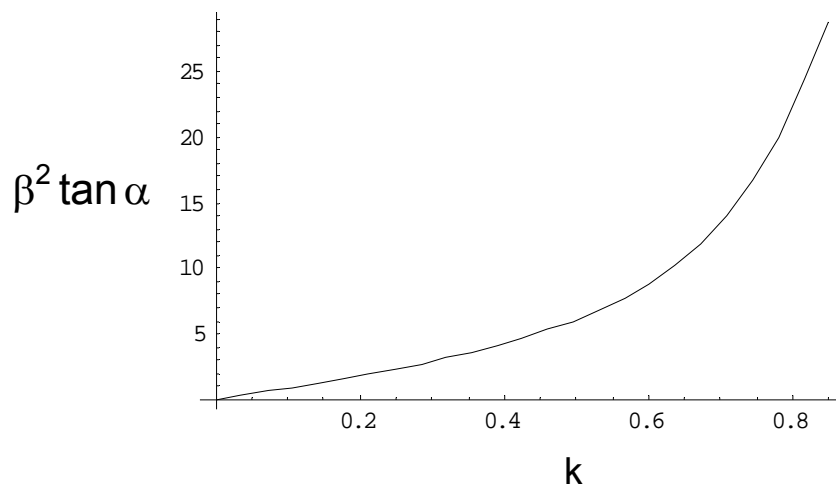


Fig. 5.  $\beta^2 \tan \alpha$  ( $= \frac{Rl^2}{EI}$ ) as a function of  $k$

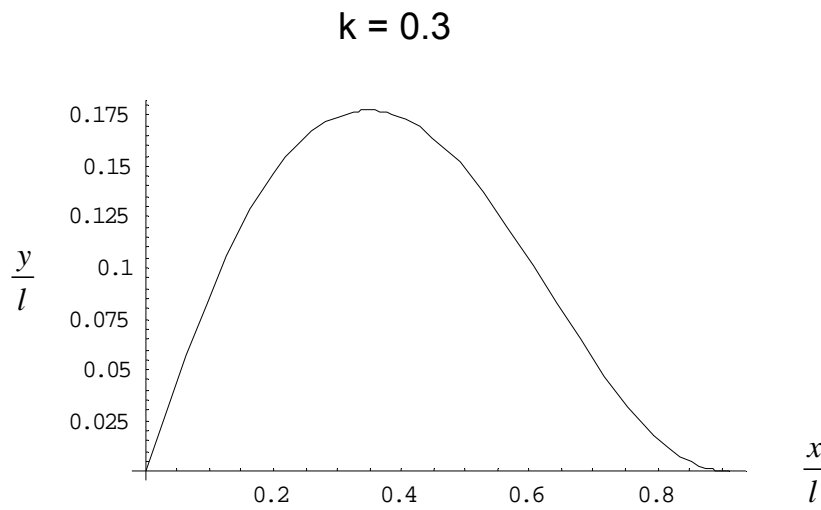


Fig. 6-1. Non-dimensionalized deformation of the beam when  $k = 0.3$

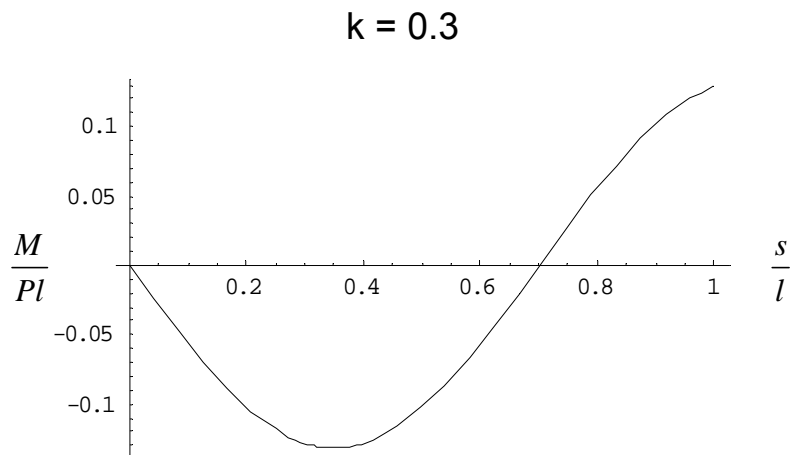


Fig. 6-2. Non-dimensional bending moment along the buckled beam when  $k = 0.3$



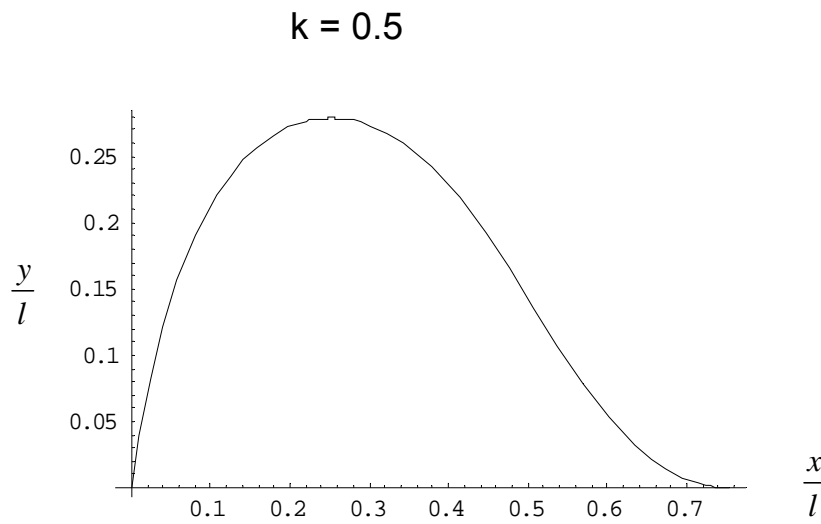


Fig. 7-1. Non-dimensionalized deformation of the beam when  $k = 0.5$

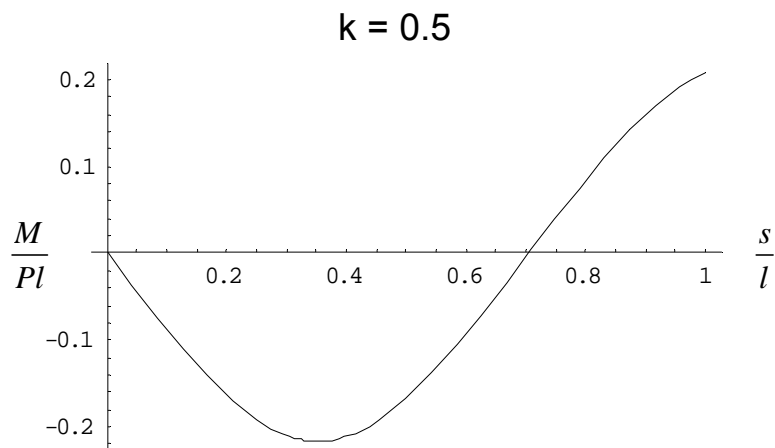


Fig. 7-2. Non-dimensional bending moment along the buckled beam when  $k = 0.5$

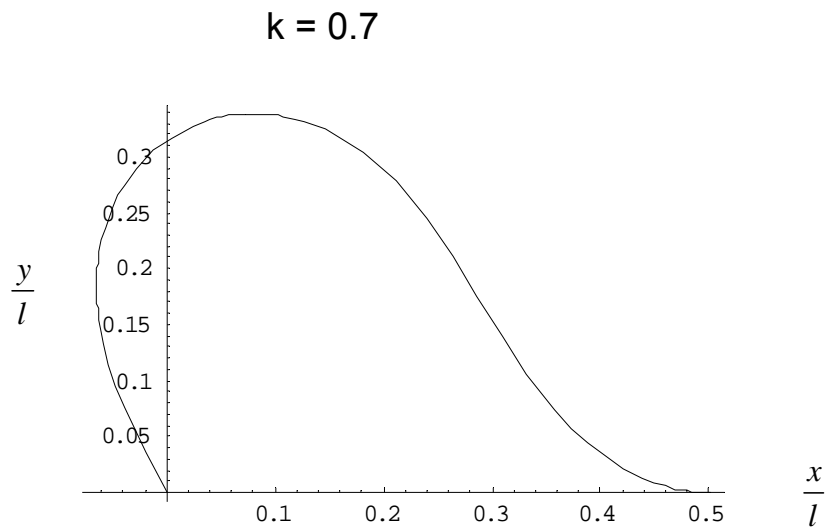


Fig. 8-1. Non-dimensionalized deformation of the beam when  $k = 0.7$

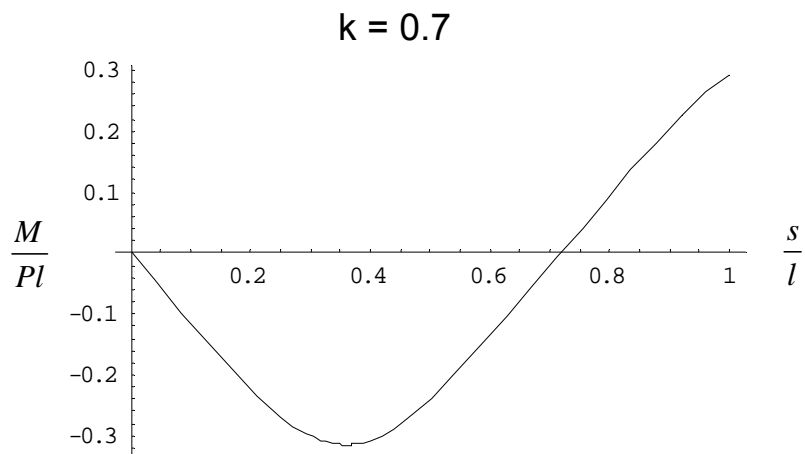


Fig. 8-2. Non-dimensional bending moment along the buckled beam when  $k = 0.7$

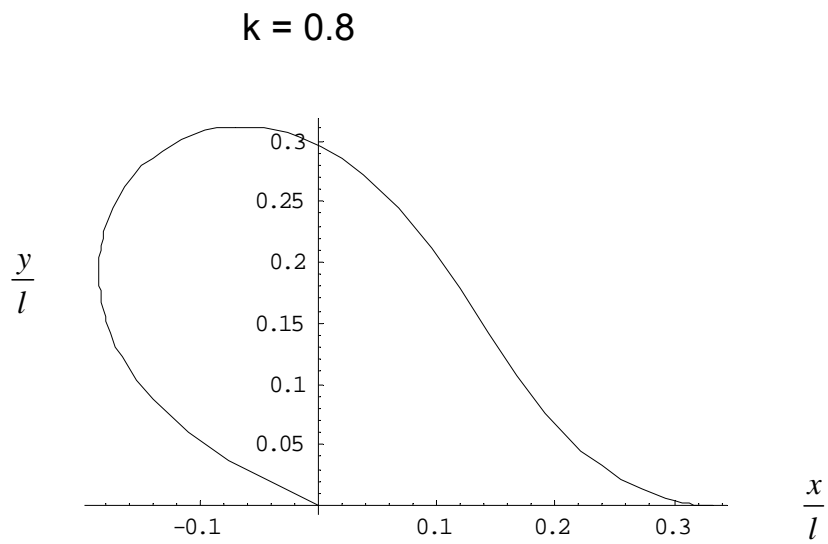


Fig. 9-1. Non-dimensionalized deformation of the beam when  $k = 0.8$

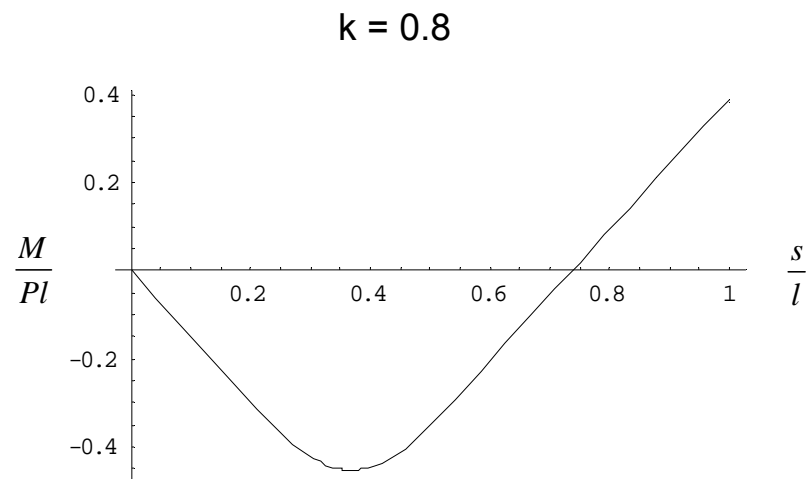


Fig. 9-2. Non-dimensionalized bending moment along the buckled beam when  $k = 0.8$